Research Square

Preprints are preliminary reports that have not undergone peer review.
They should not be considered conclusive, used to inform clinical practice,
or referenced by the media as validated information.

A Prognostic Necroptosis-Related lncRNA Signature to Predict the Immune Response and Drug Sensitivity of Bladder Cancer

Xintong Zhang
The Northern Guangdong People's Hospital Affiliated to Shantou University
Yue Lv (lvyueminiao@163.com)
First Affiliated Hospital of Harbin Medical University
Youcheng Xiu
First Affiliated Hospital of Harbin Medical University
Zan Liu
First Affiliated Hospital of Harbin Medical University

Research Article

Keywords: necroptosis, lncRNA, bladder cancer, immune, drug

Posted Date: February 10th, 2022

DOI: https://doi.org/10.21203/rs.3.rs-1339521/v1

License: This work is licensed under a Creative Commons Attribution 4.0 International License.
Read Full License

Abstract

Background: Necroptosis plays a key role in cancer treatment. Mounting evidence suggests that many kinds of drugs can promote necroptosis in various tumor cells. Patients with bladder cancer (BLCA), especially those with advanced stage cancer, have a short life span; thus, new drugs need to be developed urgently to improve the situation. Long noncoding RNAs (lncRNAs) are considered regulatory targets for cancer, including BLCA. Therefore, we constructed a promising signature of lncRNAs related to necroptosis and further predicted the immune response and sensitivity of drugs.

Methods: We downloaded the transcriptome and clinical data for BLCA from the Cancer Genome Atlas （TCGA）. The expression network was constructed using coexpression analyses. Necroptosis related to lncRNAs (nrlncRNAs) was subsequently identified by univariate Cox regression. We then constructed the signature by performing the least absolute shrinkage and selection operator(LASSO) and evaluated it by Kaplan–Meier analysis, multivariate Cox regression, time-dependent receiver operating characteristics (ROC), nomogram, calibration curves, gene set enrichment analyses(GSEA), immune checkpoint, tumor microenvironment(TME), N6-methyladenosine (m6A) modification genes, and the half-maximal inhibitory concentration (IC50) analysis in the risk groups. The set was then divided into two groups according to nrlncRNAs expression in the different types.

Results: We analyzed the survival features and principal component analysis (PCA) between the two groups. A 11-nrlncRNAs (AC008750.1, AL133297.1, AC005479.1, AP003559.1, UBE2Q1-AS1, MIR100HG, LINC02709, AC005387.1, LINC00649, AC021321.1, ETV7-AS1) prognostic signature was constructed. There was a significant difference in overall survival (OS) between the high-and low-risk groups ($p < 0.001$). The ROC curve exhibited the robust prognostic features of the signature. In addition, immune checkpoint analysis revealed that the expression of most of the immune genes in the high-risk group was higher than those in the low-risk group. FTO, ALKBH5, METTL3, and YTHDC1 were significantly different between the high-and low-risk groups in m6A regulators. The signature predicted different IC50 values to have statistical significance in high-and low-risk groups for multiple drugs, including cisplatin, docetaxel, gefitinib, and imatinib.

Conclusions: In conclusion, our constructed signature may contribute to the prognosis of patients with BLCA as well as serve as clinical predictors of chemotherapy and immunotherapy.

1 Introduction

Bladder cancer (BLCA), with an estimated 550,000 new cases and 20,000 deaths in 2018, is one of the most common malignancies in the world, accounting for a large proportion of cancer deaths in men[1]. It can be broadly classified into nonmyometrial infiltrating BLCA (NMIBC) and muscle infiltrating BLCA (MIBC), with 25% of cases diagnosed as MIBC[2, 3]. The traditional treatment option for NMIBC is transurethral bladder tumor resection (TURBT). Radical cystectomy combined with chemotherapy is the primary treatment for MIBC[4]. Recently, immune checkpoint inhibitors, antibody-drug conjugates,

and targeted therapies have gradually become options for certain patients[5]. Multiple trials have demonstrated that checkpoint inhibitors in advanced BLCA, including avelumab, atezolizumab, durvalumab, and nivolumab exert therapeutic effects by targeting the PD1/PD-L1 pathway. However, <50% of the patients showed sensitivity to checkpoint inhibitors. It has been found that tumors seem to promote the formation of an immunosuppressive microenvironment via various mechanisms to resist immunotherapy[6]. Therefore, it is a new research direction to find gene targets for improving TME and promoting immunotherapy.

Apoptosis has long been recognized as a powerful anticancer agent, but its resistance usually results in chemotherapy failure. Finding new nonapoptotic forms of programmed cell death (PCD) is imperative [7]. Necroptosis is also a type of PCD, and over the years, it has been shown to be triggered by a variety of stimuli, including Toll-like receptors(TLRs), death and interferon(IFN) receptor ligands, and certain pathogens[8]. Shikonin, a pyruvate kinase M2 (PKM2) inhibitor, can improve cisplatin resistance through BLCA cell necroptosis [9].Necroptosis is tightly regulated, requiring activation of the receptor-interacting protein (RIP) kinases RIPK1 and RIPK3. Necroptosis cells activated RIPK3 phosphorylates mixed lineage kinase domain-like protein(MLKL), which can oligomerize and translocate to the plasma membrane, resulting in the permeabilization of the necrotic plasma membrane and release of damage-related molecular patterns(DAMPs) that evoke the immune response[10]. Hence, necroptosis is referred to as an immunogenic cell death (ICD). It may be another beneficial factor in tumor clearance and/or malignancy restriction, depending on the stimulation of ICD in the TME[11]. Vaccinia virus (VV) can activate necroptosis and promote the induction of T cell-mediated immune responses[12].

LncRNAs are RNA transcripts of >200 nucleotides in length and have secondary and tertiary structures. These allow them to perform functions similar to those of proteins[13]. LncRNAs play an essential role in cancer. Genome-wide expression patterns in tumor samples have identified a large number of lncRNAs associated with various types of cancer. LncRNA expression and its mutations may maintain or regulate tumor characteristics, such as proliferation and metastasis. LncRNAs have promising prospects as novel biomarkers and therapeutic tagets for cancer[14]. At present, the role of nrlncRNAs in BLCA cells has not been studied. This study aimed to provide a new therapeutic target for BLCA resistant to chemotherapy or immunotherapy.

2 Materials And Methods

2.1 Patients and datasets

To obtain a matrix of BLCA data, we downloaded clinical data and BLCA FPKM–standardized RNA transcriptome datasets (HTSeq—FPKM) from the TCGA website (https://portal.gdc.cancer.gov/): normal count, 19 and tumor count, 414. The RNA transcript data were arranged into gene symbols and each sample gene expression matrix using Strawberry Perl for further study. Futime, fustat, age, gender, grade, and stage (T, N, and M) for each sample were extracted from clinical data. Patients with BLCA with OS of <30 days were excluded from the study.

2.2 Identification and correlation analysis of nrlncRNAs and network construction

We identified 67 genes associated with necroptosis from previous reports[15] (Appendix Table 1). First, we distinguished lncRNAs and mRNAs and explored the correlation between necroptosis gene and lncRNA expression. The “limma” R package (Pearson correlation coefficients >0.4 and *p value* < 0.001) was used to screen out highly correlated 1131 nrlncRNAs. Using the “igraph” R package, an interaction network was established to show the relationship between lncRNAs and necroptosis genes (NRGs).

2.3 Analysis of differentially expressed nrlncRNAs and risk signature construction

We used log 2 fold change (FC) > 1 and false discovery rate (FDR) < 0.05 as screening criteria to obtain the differentially expressed nrlncRNAs. NrlncRNAs related to survival ($p < 0.05$) were screened by univariate Cox regression analysis based on downloaded clinical data. Next, we ran 1,000 cycles to obtain the model gene set through Lasso regression with a *p* value of 0.05, and 10-fold cross-validation. A model was constructed after 1,000 random stimuli per cycle. The forest map was drawn using the result of the ggplot2 R package, and then the receiver operating characteristics (ROC) curves of the mode were plotted. We calculated the risk score for all samples using the following formula: . represents the coefficient of nrlncRNAs that correlate with survival. indicates the expression levels of nrlncRNAs. The BLCA samples were divided into high-and low-risk groups based on the median risk score. The different OS times between the two groups were analyzed using Kaplan–Meier plotter and R packet “survival.”

2.4 Independence factor analysis

Univariate and multivariate Cox regression analyses were performed to assess whether risk score and clinical features were independent factors, and the different factors were compared by ROC analysis.

2.5 Nomogram

We used the rms R package to construct the nomogram including risk score, age, gender, and stage (T, N, and M) to predict the 1-, 3-, and 5-year OS rates of patients with BLCA. We used a calibration curve based on the Hosmer–Lemeshow test to examine whether the predicted outcome was consistent with the practical outcome.

2.6 Gene set enrichment analyses (GSEA)

GSEA was performed using the GSEA 4.2.1. Enriched pathways ($p < 0.05$ and FDR < 0.25) were considered between the low- and high-risk groups.

2.7 Immune, TME, and M6A analyses

The immune cells and immune pathways were estimated using single-sample GSEA (ssGSEA). We downloaded the tumor immune cell infiltration file from TCGA. We subsequently calculated the sample's immune cell infiltration status including XCELL, TIMER, CIBERSORT, QUANTISEQ, MCPCOUNTER, EPIC, and CIBERSORT-ABS on TIMER2.0 (http://timer.cistrome.org/) and mapped the bubbles. We also compared immune checkpoint activation and TME scores between the low-risk and high-risk groups using ggplot2 , ggpubr and estimated R packages. We collated 13 M6A regulatory factors from previously published studies. (Appendix Table 2). The m6A-related gene expression of high and low-risk groups were compared using the limma, reshape2, ggplot2, and ggpubr R packages.

2.8 Drug sensitivity

Next, we used the pROphetic R package to assess drug sensitivity between high- and low-risk groups by comparing the half-maximal inhibitory concentration (IC50) of each patient with BLCA with Genomics of Drug Sensitivity in Cancer (https://www.cancerrxgene.org/)[16].

2.9 Tumor cluster

Potential clusters between tumor samples were explored using the ConsensusClusterPlus (CC) R package based on prognostic 11-lncRNA expression. Principal component analysis (PCA) was performed using the Rtsne R package. Differences in immune cell infiltration, immunocheckpoint, TME, and drug sensitivity analyses were compared among the BLCA sample clusters.

3 Results

3.1 Identification of necroptosis-related lncRNAs in patients with BLCA

The study workflow is illustrated in Figure 1. In this study, we used data from 433 patients with BLCA from the TCGA cohort (T = 414, $N = 19$). After finding all lncRNAs and establishing coexpression analysis with 67 NRGs to identify lncRNAs related to necroptosis (coefficients >0.4 and $p < 0.001$), we established an interactive network to demonstrate the relationship between nrlncRNAs and NRGs (Figure 2A). Next, 686 nrlncRNAs with significant differences were identified by differential expression analysis (FC > 1 and FDR < 0.05). We found that 108 nrlncRNAs were downregulated, while the others were upregulated,

mapping the volcano plot (Figure 2B). We selected up-and downregulated nrlncRNAs of the top 50 most significant differences in the heat map (Figure 3B).

3.2 Construction of prognostic necroptosis-related lncRNAs signature

According to univariate Cox regression analysis, nrlncRNAs related to survival ($p < 0.05$) were screened and plotted on forest map (Figure 3A). The Sankey diagram illustrates the regulatory relationship between these lncRNAs and NRGs (such as TSC1, BRAF, and ATRX) (Figure 3B). To avoid over-fitting of the signature, when the first value of Log (λ) was the minimum possible deviance, we performed LASSO regression and multiple Cox regression analysis on these nrlncRNAs (Figure 4A and B). Finally, an 11-necroptosis-related lncRNA signature was established.

Risk score was calculated using the following formula: Risk score = (AC008750.1 × -2.18520147058094)+(AL133297.1 × 2.05280592077303)+(AC005479.1 × 1.35382239745128)+ (AP003559.1 × 1.28533807015561) + (UBE2Q1-AS1 × -1.16093696050806) + (MIR100HG × 0.449749505941033) + (LINC02709 × 1.25314467417777) + (AC005387.1 × -0.607382896530388) + (LINC00649 × -0.490052688800663) + (AC021321.1 × -1.16608863558295) + (ETV7-AS1 × -0.589464760152836) (Table 1). Patients were further divided into high- and low-risk groups, with the median risk score as the standard. When the model was constructed, we divided the samples into two groups (train and test) and obtained OS analysis, risk score curve, survival status, and 11-nrlncRNAs risk heat map (Figure 5A–C).

Univariate and multivariate Cox regression analyses were used to compare the risk scores of the signature with age, gender, grade, and stage (Figure 6A and B). Area under the ROC curve (AUC) of 1-, 3-, and 5-years survival were 0.736, 0.735, and 0.744, respectively, and AUCs of the risk score (0.736) compared with other factors including age (0.662), gender(0.479), grade (0.529), and stage (0.641), respectively (Figure 6C and D).

3.3 Nomogram

We divided patients with BLCA into stage I/II and stage III/IV groups, and then compared whether OS (survival probability) of patients in high-or low-risk groups had significant differences in the two stages according to the risk score of the model. We built a nomogram for predicting the 1-, 3-, and 5-year survival rates of patients with BLCA and plotted the 1-, 3-, and 5-year calibration curves (Figure 6 E–I).

3.4 GSEA

To investigate the functional and enrichment pathway differences between high-and low-risk groups, we used GSEA software to explore the Kyoto Encyclopedia of Genes and Genomes pathway throughout the entire set. The high-and low-risk groups enriched the first five pathways, and the BLCA pathway was built using multiple GSEA. The BLCA pathway (p 0.01 < 0.05; FDR 0.044< 0.25; |NES| 1.78> 1.5) was significant in the risk group of this model (Figure 7A and B) (Appendix Figure 1A)

3.5 Immunity factors, TME, and M6A analyses in risk groups

The relationship between immune cells and the patient's risk score is depicted in the immune cell bubble chart (Figure 7C). Cancer-associated fibroblast_XCELL, endothelial cell_MCP-counter, granulocyte-monocyte progenitor XCELL, macrophage M1_QUANTISEQ, macrophage M2_CIBERSORT, etc. were positively correlated with BLCA patients'risk scores (p < 0.05). However, B cell memory CIBERSORT, B cell_TIMER, T cell CD4+ central memory_XCELL, T cell CD8+ naive_XCELL, and regulatory T cells (Tregs)_CIBERSORT-ABS, among others, showed a negative correlation(p < 0.05) (Figure 7C). Specific correlation coefficients and p-values for each type of immune cell are shown in Appendix Figure 1B and Appendix Table 3. SSGSEA showed that there were significant differences in immune cells such as macrophages, mast cells, neutrophils, Th1-cells, and Treg and immune-related function scores such as APC-co-inhibition and APC-co-stimulation between high- and low-risk groups, respectively (p < 0.001) (Figure 7D and E). Stromal cells, immune cells, and composite scores of each BLCA sample are shown, and the differences in these scores were compared between the high- and low-risk groups (p < 0.05) (Figure 7F–H). We found higher immune checkpoint gene expression in the high-risk group. There were significant differences in the expression of many genes, such as CD274, CD44, CD276, and HAVCR2, between the high-and low-risk groups (Figure 7I). Significant differences were found in multiple m6A regulators gene expression in risk groups such as FTO, ALKBH5, METTL3, and YTHDC1 (Figure 7G).

3.6 Distinguishing BLCA clusters and cluster evaluation

We performed nine cluster comparisons of BLCA samples and found the weakest correlation between the two subtypes. We divided the BLCA samples into two distinct subtypes (C1 and C2) (Appendix Figure 2). There are usually differences in immunotherapy and survival analysis between the C1and C2 subtypes[17] (Figure 8A). We observed a significant difference in survival probability between C1 and C2 (p = 0.032) (Figure 8B). In addition, we used the ggalluvial graph to show the relationship between high/low risk groups and C 1/C 2 clusters (Figure 8C). PCA analysis showed that the expression of lncRNAs in BLCA could be used to scatter the sample clusters (C1 and C2) (Figure 8D and E).

The differences in stromal cells, immune cells, and composite scores in each BLCA sample were compared between the C1 and C2 groups (p < 0.05) (Figure 8F–H). Heat map revealed differences among different immune cells in the tumor clusters. T cell CD4+_TIMER, T cell CD8+_TIMER, and Neutrophil_TIMER immune cells were highly concentrated in the C1 cluster (Figure 8I). Immune

checkpoint gene expressions such as TNFRSB4, CD274, and CD70 were mostly higher in the C1 cluster than in the C2 cluster (Figure 8J).

3.7 Drug sensitivity

The IC50 of many chemotherapeutic or targeted drugs showed significant differences between the high- and low-risk groups of the prognostic signature. This also suggests that the use of this model to differentiate patients can improve drug sensitivity to some extent and avoid drug resistance, especially some commonly used chemotherapeutic or targeted drugs such as cisplatin, dasatinib, docetaxel, gefitinib, imatinib, nilotinib, methotrexate, and lenalidomide (Figure 8A). The same pattern was predicted for the C1 and C2 clusters (Figure 8B).

4 Discussion

Cancer chemotherapy can no longer depend on a single drug treatment, such as cisplatin, as one chemotherapy drug cannot work for all patients and be 100% effective against cancer progression. Resistance to anticancer drugs is caused by a number of factors, including individual differences that make resistance to chemotherapy more common[18]. Clinically, the survival rates for patients with advanced or metastatic BLCA remain low[19]. Thus, more attention should be paid to individualized treatment of patients. The establishment of a prognostic signature plays a key role. We developed an 11-nrlncRNAs prognostic signature that could classify the BLCA samples into high- and low-risk groups and further evaluate the differences between the two groups, including survival analysis ($p < 0.05$), immunity factors, TME, and M6A analysis. We hope that this model will provide a new treatment strategy for BLCA.

The inhibitory role of necroptosis in cancer has been extensively studied. However, very few cases of BLCA have been reviewed. The PKM2 inhibitor shikonin, a PKM2 inhibitor, can overcome cisplatin resistance and promote necroptosis[9]. ABT 737, a bcl-2 family inhibitor, can also induce necroptosis in BLCA cells[20]. There may also be crosstalk between necroptosis and other forms of PCD, such as ferroptosis or pyroptosis[21]. Researchers constructed a 9-ferroptosis-related lncRNAs model to predict the prognosis of patients with BLCA and found that they were more sensitive to anti-PD-1/L1 immunotherapy and chemotherapy drugs, such as sunitinib, paclitaxel, docetaxel, and docetaxel[22]. Recently, an 8-nrlncRNAs prognostic signature associated with pyroptosis was developed to explore the molecular markers of BLCA[23]. We recently constructed a model of necroptosis, according to which the samples were scored and divided into high-and low-risk groups. High-risk patients were found to be more sensitive to a variety of drugs such as cisplatin, dasatinib, docetaxel, and imatinib. It also provides a direction for our clinical treatment to rely on this model. In addition, we also found that diverse drugs have different sensitivities to tumor clusters.

Immunotherapy has been widely used in clinical and scientific research in recent years. The main benefit of immune checkpoint inhibitor-related drugs over conventional chemotherapy is that patients with BLCA are more resistant to them and lead to a reduction in adverse events. Unfortunately, the response rate to

immune checkpoint inhibitor is relatively low[24]. Immune function scores including APC_co_inhibition, APC_co_stimulation, CCR, checkpoint, T_cell_ co_ stimulation, and parainflammation were significantly different between the high-and low-risk groups. Thus, we can explore which immune checkpoints are more beneficial to the patient based on the patient's classification. CD274, CD44, HAVCR2, PDCD1LG2, LAIR1, CD276, TNFSF9, TNFRSF8, CD86, TNFRSF4, NRP1, and CD80 were highly expressed in the high-risk group. CD274 (PD-L1 promoter gene) methylation is an independent prognostic factor for BLCA[25]. CD44 is a surface marker of cancer stem cells and has also been found to be associated with drug resistance to BLCA treatment[26]. Conversely, TNFRSF14, TNFRSF25, CD160, LGALS9, andTMIGD2 were highly expressed in the low-risk group. The increased expression of TNFRSF14 can inhibit the growth of BLCA cells[27]. This suggests that our prognostic model is useful for BLCA classification and individualized treatment. Examining the immune checkpoint sensitivity of different BLCA samples may improve the response rate to immunotherapy.

M6A is the most common methylation modification and plays an essential role in lncRNA expression stability[28]. In this study, m6A regulator (FTO, ALKBH5) gene expression was higher in the high-risk group ($p < 0.001$). The expression of METTL3 and YTHDC1 was higher in the low-risk group ($p < 0.001$). FTO can promote BLCA growth by regulating the MALAT/miR-384/MAL2 axis by M6A RNA modification[29]. ALKBH5 has been shown to inhibit BLCA cell proliferation and sensitize cells to cisplatin by m6A-casein kinase 2 (CK2)α[30]. Therefore, the role of m6A methylase is more dependent on downstream genes in BLCA.

The limitations of this study include the lack of experimental evidence for the role of 11-nrlncRNAs (AC008750.1, AL133297.1, AC005479.1, AP003559.1, UBE2Q1-AS1, MIR100HG, LINC02709, AC005387.1, LINC00649, AC021321.1, and ETV7-AS1) in BLCA. LINC00649 has been found to promote the malignant progression of BLCA cells via the miR-15a-5p/HMGA1[31] and miR-16-5p/JARID2[32] axes. The roles of other nrlncRNAs still need to be explored further in the future.

5 Conclusions

In conclusion, our constructed signature may contribute to the prognosis of patients with BLCA as well as serve as clinical predictors of chemotherapy and immunotherapy.

Abbreviations

lncRNA : long non-coding RNA

BLCA : bladder cancer

TCGA : the Cancer Genome Atlas

nrlncRNAs : necroptosis related to lncRNAs

LASSO : least absolute shrinkage and selection operator

ROC : receiver operating characteristics

GSEA : gene set enrichment analyses

m6A : N6-methyladenosine

IC50: the half-maximal inhibitory concentration

PCA : principal component analysis

OS : overall survival

NMIBC : non-myometrial infiltrating bladder cancer

MIBC : muscle infiltrating bladder cancer

TURBT : transurethral bladder tumor resection

TME : tumor microenvironment

PCD : programmed cell death

TLRs: Toll-like receptors

IFN : interferon

PKM2: pyruvate Kinase M2

RIP : receptor-interacting protein

MLKL : mixed lineage kinase domain-like protein

DAMPs : damage-related Molecular Patterns

ICD : immunogenic cell death

ssGSEA : single-sample gene set enrichment analysis

GDSC : Genomics of Drug Sensitivity in Cancer

CC : ConsensusClusterPlus

NRGs : necroptosis genes

AUC: Area Under ROC Curve

CK2: casein kinase 2

Declarations

Competing interests

The authors declare that the research was conducted in the absence of any commercial or financial relationships that could be construed as a potential conflict of interest.

Author Contributions:

XZ and YL wrote the first draft of the manuscript. ZL and YL designed and modified this study. YX provided guidance throughout the preparation of this manuscript. All authors contributed to the article and approved the submitted version.

Data Availability

The data supported the results are available at the TCGA (https://tcga-data.nci.nih.gov/tcga/) and GDSC (https://www.cancerrxgene.org/). The original contribution can be directed to the corresponding author in the study.

Funding

Not applicable

Acknowledgements

Not applicable

Consent for publication

Authors' information

Xintong Zhang Department of neurosurgery, The Northern Guangdong People's Hospital Affiliated to Shantou University Shaoguan 512026 Guangdong, China.

Yue Lv, Youcheng Xiu, Zan Liu Department of Urology, The First Affiliated Hospital, Harbin Medical University, Harbin 150000, Heilongjiang, China.

Xintong Zhang and Yue Lv have contributed equally to this work and share first authorship

Correspondence: lvyueminiao@163.com youchengxiu2000@163.com; Liuzan@hrbmu.edu.cn

Ethics Approval and Consent to Participate

Not applicable.

Consent for publication

Not applicable.

Additional information

Publisher's Note

Springer Nature remains neutral with regard to jurisdictional claims in published maps and institutional affiliations.

References

1. Bray, F., et al., *Global cancer statistics 2018: GLOBOCAN estimates of incidence and mortality worldwide for 36 cancers in 185 countries.* CA Cancer J Clin, 2018. **68**(6): p. 394-424.
2. Dobruch, J., et al., *Gender and Bladder Cancer: A Collaborative Review of Etiology, Biology, and Outcomes.* Eur Urol, 2016. **69**(2): p. 300-10.
3. Cumberbatch, M.G.K., et al., *Epidemiology of Bladder Cancer: A Systematic Review and Contemporary Update of Risk Factors in 2018.* Eur Urol, 2018. **74**(6): p. 784-795.
4. DeGeorge, K.C., H.R. Holt, and S.C. Hodges, *Bladder Cancer: Diagnosis and Treatment.* Am Fam Physician, 2017. **96**(8): p. 507-514.
5. Lenis, A.T., et al., *Bladder Cancer: A Review.* Jama, 2020. **324**(19): p. 1980-1991.
6. Crispen, P.L. and S. Kusmartsev, *Mechanisms of immune evasion in bladder cancer.* Cancer Immunol Immunother, 2020. **69**(1): p. 3-14.
7. Gong, Y., et al., *The role of necroptosis in cancer biology and therapy.* Mol Cancer, 2019. **18**(1): p. 100.
8. He, S., et al., *Toll-like receptors activate programmed necrosis in macrophages through a receptor-interacting kinase-3-mediated pathway.* Proc Natl Acad Sci U S A, 2011. **108**(50): p. 20054-9.
9. Wang, Y., et al., *PKM2 Inhibitor Shikonin Overcomes the Cisplatin Resistance in Bladder Cancer by Inducing Necroptosis.* Int J Biol Sci, 2018. **14**(13): p. 1883-1891.
10. Zhu, F., et al., *Complex roles of necroptosis in cancer.* J Zhejiang Univ Sci B, 2019. **20**(5): p. 399-413.
11. Scarpitta, A., et al., *Pyroptotic and Necroptotic Cell Death in the Tumor Microenvironment and Their Potential to Stimulate Anti-Tumor Immune Responses.* Front Oncol, 2021. **11**: p. 731598.
12. Ma, J., et al., *Characterization of virus-mediated immunogenic cancer cell death and the consequences for oncolytic virus-based immunotherapy of cancer.* Cell Death Dis, 2020. **11**(1): p. 48.
13. Novikova, I.V., S.P. Hennelly, and K.Y. Sanbonmatsu, *Tackling structures of long noncoding RNAs.* Int J Mol Sci, 2013. **14**(12): p. 23672-84.
14. Bhan, A., M. Soleimani, and S.S. Mandal, *Long Noncoding RNA and Cancer: A New Paradigm.* Cancer Res, 2017. **77**(15): p. 3965-3981.

15. Zhao, Z., et al., *Necroptosis-Related lncRNAs: Predicting Prognosis and the Distinction between the Cold and Hot Tumors in Gastric Cancer.* J Oncol, 2021. **2021**: p. 6718443.
16. Geeleher, P., N.J. Cox, and R.S. Huang, *Clinical drug response can be predicted using baseline gene expression levels and in vitro drug sensitivity in cell lines.* Genome Biol, 2014. **15**(3): p. R47.
17. Das, S., K. Camphausen, and U. Shankavaram, *Cancer-Specific Immune Prognostic Signature in Solid Tumors and Its Relation to Immune Checkpoint Therapies.* Cancers (Basel), 2020. **12**(9).
18. Gottesman, M.M., *Mechanisms of cancer drug resistance.* Annu Rev Med, 2002. **53**: p. 615-27.
19. Bellmunt, J., *Bladder cancer.* Hematol Oncol Clin North Am, 2015. **29**(2): p. xiii-xiv.
20. Cheng, R., et al., *ABT-737, a Bcl-2 family inhibitor, has a synergistic effect with apoptosis by inducing urothelial carcinoma cell necroptosis.* Mol Med Rep, 2021. **23**(6).
21. Tang, R., et al., *Ferroptosis, necroptosis, and pyroptosis in anticancer immunity.* J Hematol Oncol, 2020. **13**(1): p. 110.
22. Chen, M., et al., *A New Ferroptosis-Related lncRNA Signature Predicts the Prognosis of Bladder Cancer Patients.* Front Cell Dev Biol, 2021. **9**: p. 699804.
23. Lia, T., et al., *Development and validation of Pyroptosis-related lncRNAs prediction model for bladder cancer.* Biosci Rep, 2022.
24. Bednova, O. and J.V. Leyton, *Targeted Molecular Therapeutics for Bladder Cancer-A New Option beyond the Mixed Fortunes of Immune Checkpoint Inhibitors?* Int J Mol Sci, 2020. **21**(19).
25. Xu, J., et al., *CD274 (PD-L1) Methylation is an Independent Predictor for Bladder Cancer Patients' Survival.* Cancer Invest, 2022: p. 1-6.
26. Wu, C.T., et al., *Impact of CD44 expression on radiation response for bladder cancer.* J Cancer, 2017. **8**(7): p. 1137-1144.
27. Zhu, Y.D. and M.Y. Lu, *Increased expression of TNFRSF14 indicates good prognosis and inhibits bladder cancer proliferation by promoting apoptosis.* Mol Med Rep, 2018. **18**(3): p. 3403-3410.
28. Liu, H., et al., *A novel N6-methyladenosine (m6A)-dependent fate decision for the lncRNA THOR.* Cell Death Dis, 2020. **11**(8): p. 613.
29. Tao, L., et al., *FTO modifies the m6A level of MALAT and promotes bladder cancer progression.* Clin Transl Med, 2021. **11**(2): p. e310.
30. Yu, H., et al., *ALKBH5 Inhibited Cell Proliferation and Sensitized Bladder Cancer Cells to Cisplatin by m6A-CK2α-Mediated Glycolysis.* Mol Ther Nucleic Acids, 2021. **23**: p. 27-41.
31. Chen, X. and S. Chen, *LINC00649 promotes bladder cancer malignant progression by regulating the miR-15a-5p/HMGA1 axis.* Oncol Rep, 2021. **45**(4).
32. Liu, Y., et al., *LINC00649 Facilitates the Cellular Process of Bladder Cancer Cells via Signaling Axis miR-16-5p/JARID2.* Urol Int, 2021: p. 1-9.

Tables

Table 1: The coefficients of 11-nrlncRNAs were listed.

nrlncRNA	coefficient
AC008750.1	-2.18520147058094
AL133297.1	2.05280592077303
AC005479.1	1.35382239745128
AP003559.1	1.28533807015561
UBE2Q1-AS1	-1.16093696050806
MIR100HG	0.449749505941033
LINC02709	1.25314467417777
AC005387.1	-0.607382896530388
LINC00649	-0.490052688800663
AC021321.1	-1.16608863558295
ETV7-AS1	-0.589464760152836

Figures

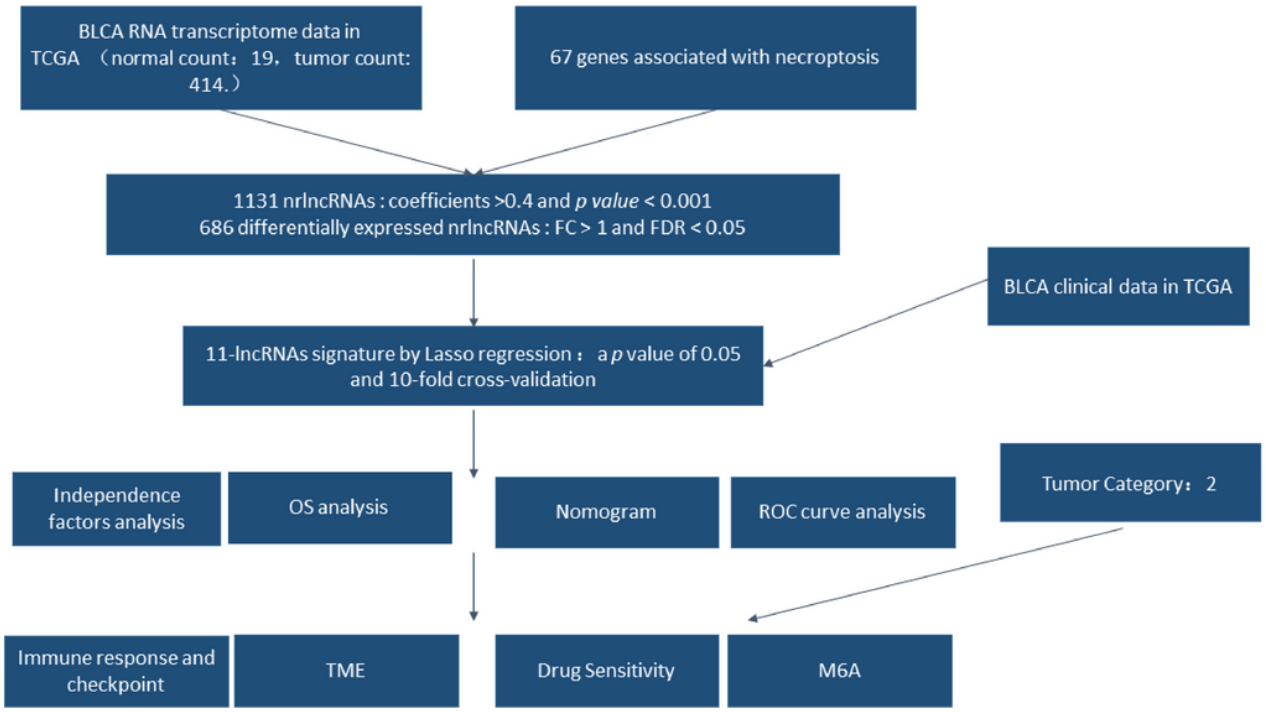

Figure 1

Study workflow

Figure 2

(A) The interactive network between lncRNAs and NRGs. **(B)** Red Dots represent (log FC > 0) upregulated genes, whereas green dots (log FC < 0) represent downregulated genes. **(C)** The expression profiles of 50 upregulated and downregulated nrlncRNAs each.

Figure 3

(A) The prognostic nrlncRNAs ($p < 0.05$) extracted by univariate Cox regression analysis. **(B)** The regulatory relationship between prognostic nrlncRNAs and NRGs was mostly positive, and only six nrlncRNAs were negative.

Figure 4

(A) The coefficient profile of prognostic nrlncRNAs in the LASSO model. **(B)** The partial likelihood deviance of the LASSO model shown by cross-validation.

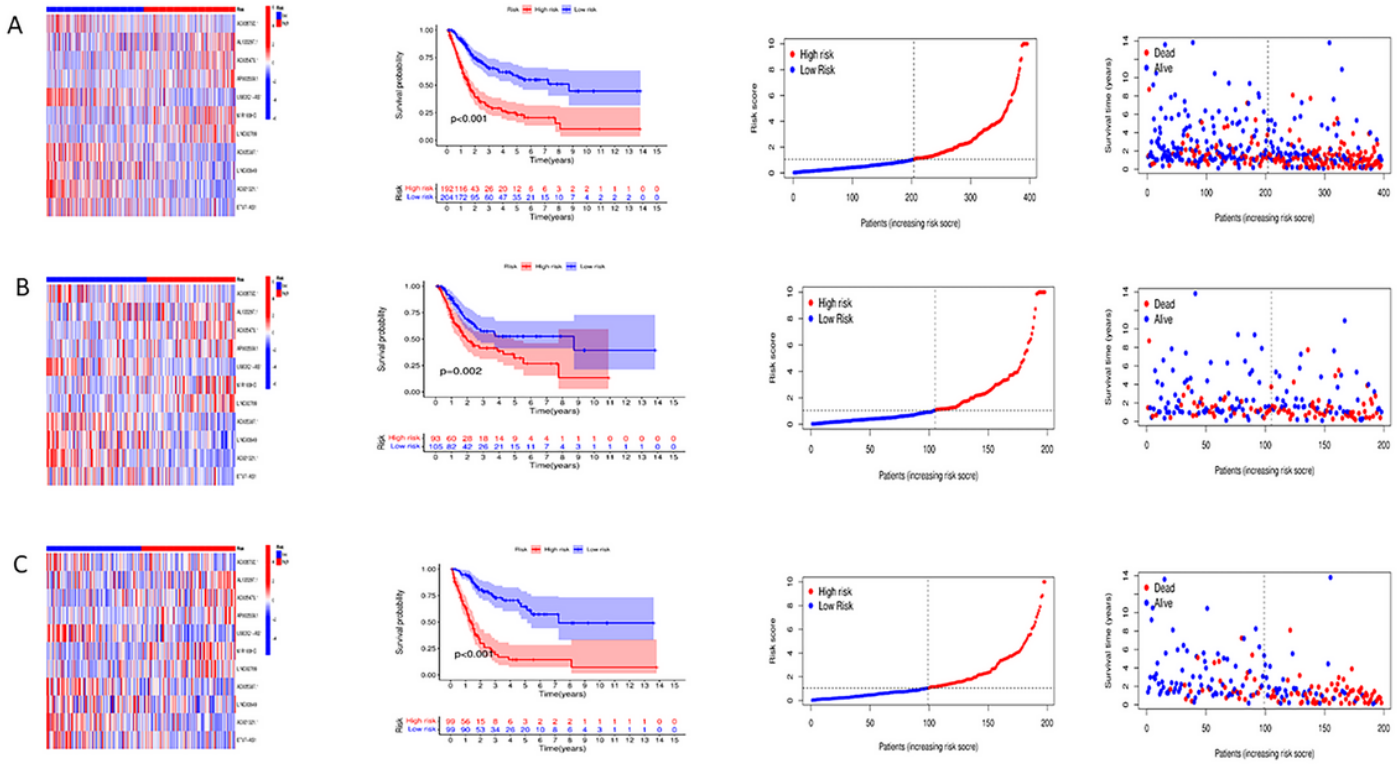

Figure 5

The exhibition of nrlncRNAs model based on 11-nrlncRNAs risk heat map, OS analysis ($p < 0.05$), risk score curve and survival status of the entire **(A)**, test **(B)**, and train **(C)** sets.

Figure 6

(A and B) Uni- and multivariate Cox analyses of risk score and clinical factors. Risk score ($p < 0.001$), age, and stage ($p < 0.001$) were statistically significant ($p < 0.05$). **(C and D)** The AUCs of 1-, 3-, and 5-years were greater than 0.7. The AUC of risk was greater than those of other clinical factors. **(E–G)** In stages I/II and III/ IV groups, OS (survival probability) between high- and low-group had significant differences ($p < 0.001$). The 1-, 3-, and 5-year OS calibration curves are shown. **(H and I)** The nomogram and calibration curves that integrated the risk score, age, gender, and tumor TNM predicted the OS probability of the 1-, 3-, and 5-year.

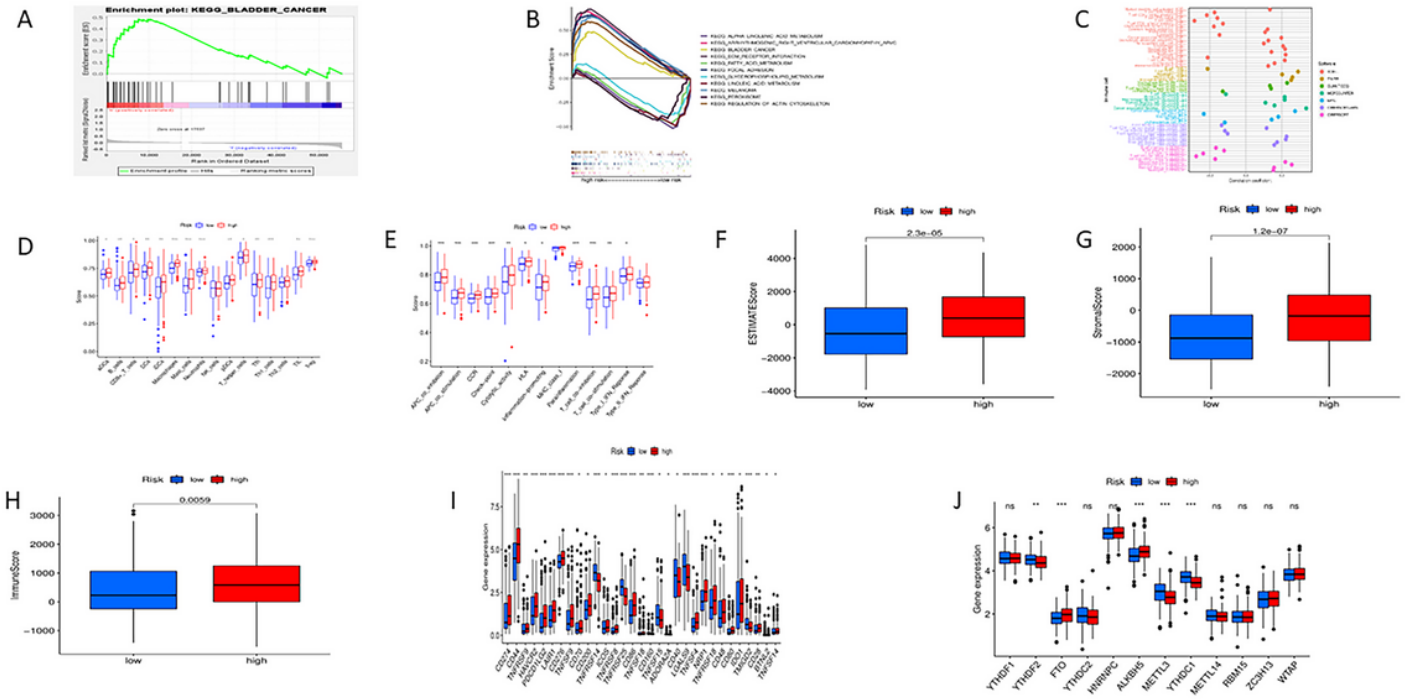

Figure 7

(A) The BLCA pathway GSEA was shown. **(B)** Multiple GSEA in risk groups. **(C)** The immune cells bubble of the relationship between the immune cells and the patient's risk score. **(D)** The SSGSEA differential expression analysis of immune cells in risk groups. **(E)** SSGSEA differential expression analysis of immune-related function scores in risk groups. **(F–H)** TME scores were compared between the high-and low-risk groups. **(I)** Immune checkpoint gene expression in risk groups. **(J)** M6A regulators gene expression in risk groups.

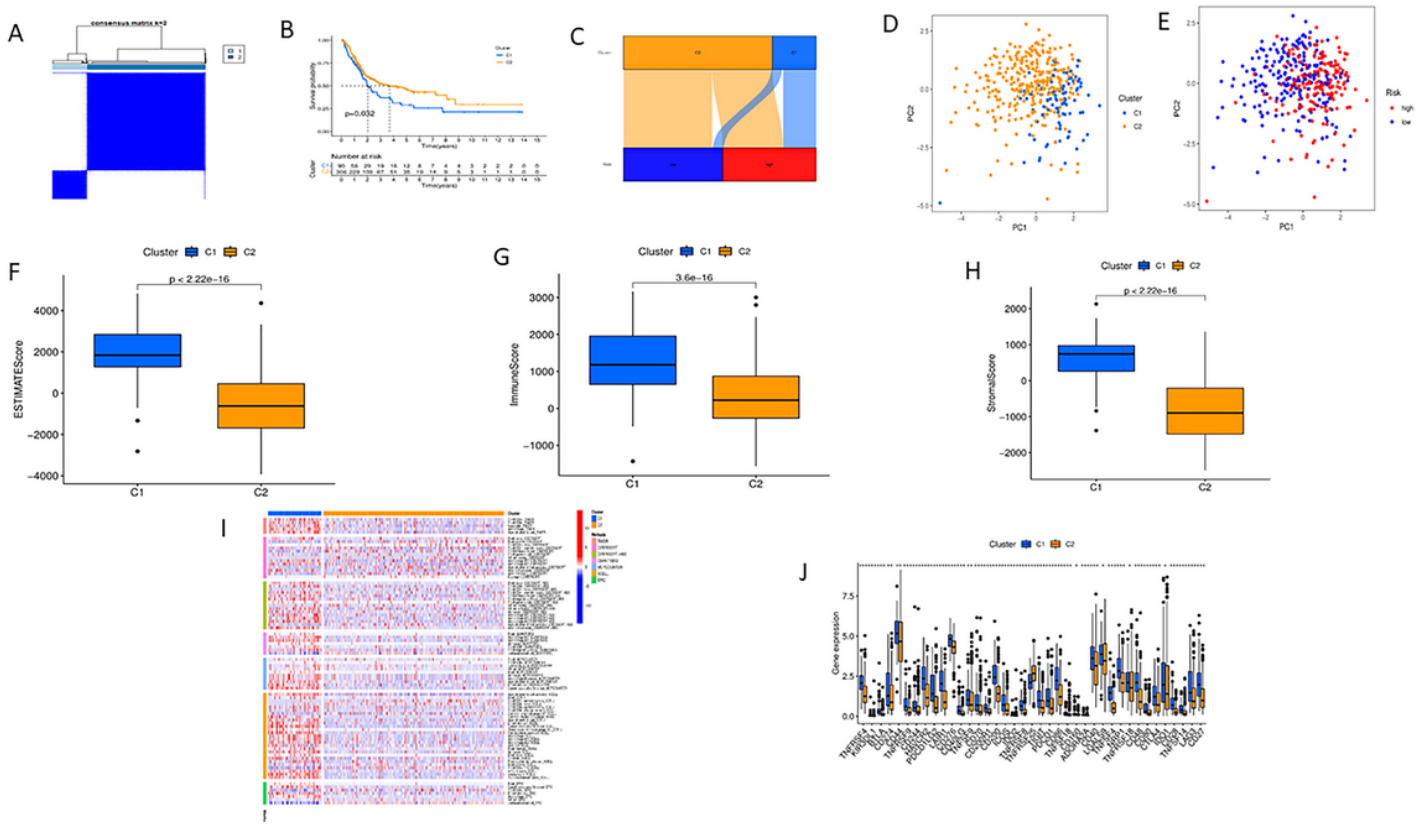

Figure 8

(A) The BLCA samples were divided into C1 and C2 clusters. **(B)** C1 and C2 clusters survival analysis. (**C**) The ggalluvial graph between risk groups and C1/C2 clusters. **(D and E)** PCA analysis in C1 and C2 clusters. **(F–H)** TME scores were compared between C1 and C2 clusters. **(I)** Heat map depicting different immune cells in the BLCA clusters. **(J)** Immune checkpoint gene expression in BLCA clusters.

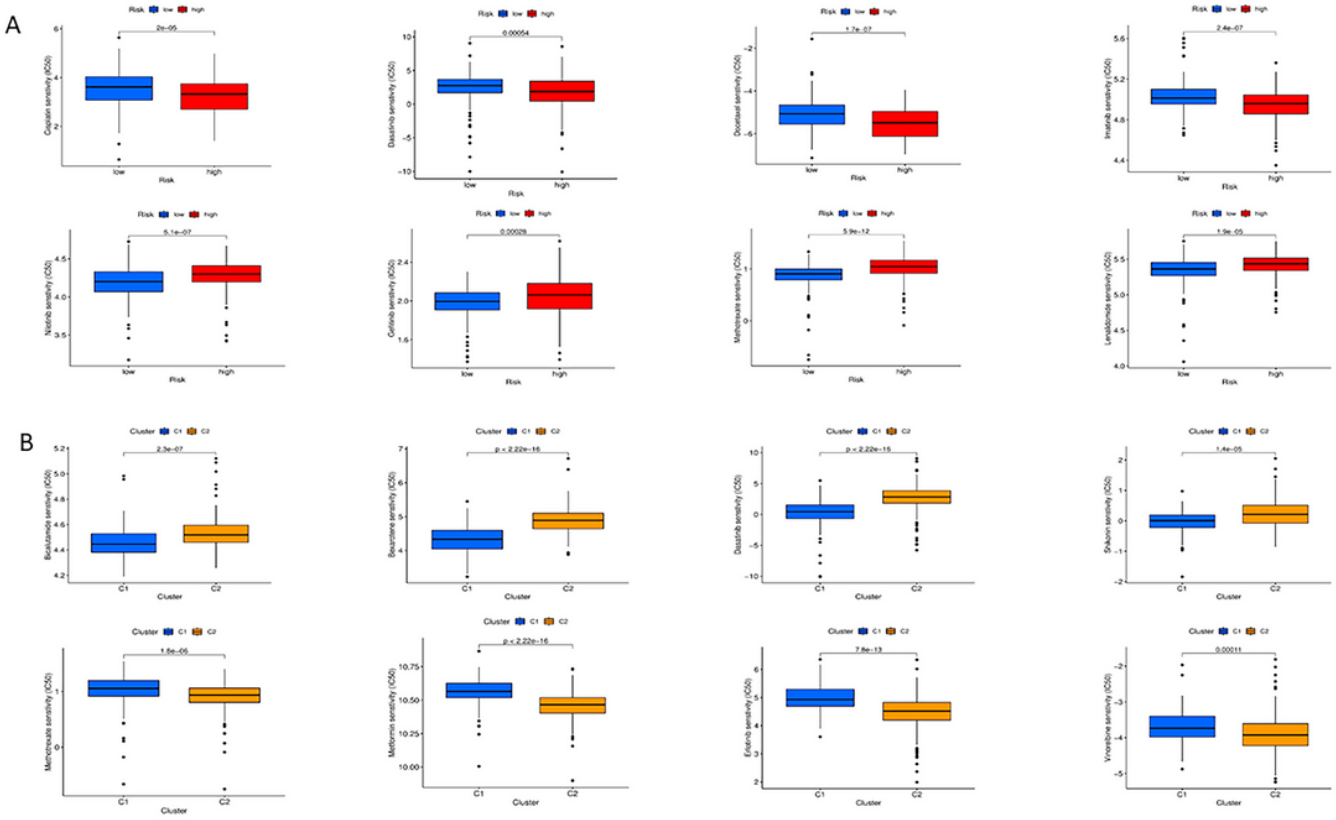

Figure 9

(A) Gefitinib nilotinib methotrexate and lenalidomide in low-risk group showed greater drugs sensitivity. Cisplatin, dasatinib, docetaxeland, and imatinib showed greater drugs sensitivity in high-risk group. **(B)** Bicalutamide, bexarotene, dasatinib, and shikonin were more sensitive in C1 cluster. However, methotrexate, metformin, erlotinib, and vinorelbine were more sensitive in C2 cluster.

Supplementary Files

This is a list of supplementary files associated with this preprint. Click to download.

- afigure1.jpg
- afigure2.jpg
- AppendixTable1.docx